Exploiting fine-scale genetic and physiological variation of closely related microbes to reveal unknown enzyme functions

Received for publication, March 19, 2017, and in revised form, June 1, 2017 Published, Papers in Press, June 7, 2017, DOI 10.1074/jbc.M117.787192

Ahmet H. Badur[‡1], Matthew J. Plutz[‡1], Geethika Yalamanchili[‡], Sujit Sadashiv Jagtap[‡], Thomas Schweder[§], Frank Unfried[§], Stephanie Markert[§], Martin F. Polz[¶], Jan-Hendrik Hehemann[‖2], and Christopher V. Rao[‡3]**

*From the [‡]Department of Chemical and Biomolecular Engineering, University of Illinois at Urbana-Champaign, Urbana, Illinois 61801, the [‖]Center for Marine Environmental Sciences University of Bremen (MARUM), Bremen 28359, Germany, the **Max Planck-Institute for Marine Microbiology, Celsiusstrasse 1, Bremen 28359, Germany, [§]Pharmaceutical Biotechnology, Institute of Pharmacy, Ernst Moritz Arndt University of Greifswald, D-17489 Greifswald, Germany, and the [¶]Department of Civil and Environmental Engineering, Massachusetts Institute of Technology, Cambridge, Massachusetts 02139*

Edited by Chris Whitfield

Polysaccharide degradation by marine microbes represents one of the largest and most rapid heterotrophic transformations of organic matter in the environment. Microbes employ systems of complementary carbohydrate-specific enzymes to deconstruct algal or plant polysaccharides (glycans) into monosaccharides. Because of the high diversity of glycan substrates, the functions of these enzymes are often difficult to establish. One solution to this problem may lie within naturally occurring microdiversity; varying numbers of enzymes, due to gene loss, duplication, or transfer, among closely related environmental microbes create metabolic differences akin to those generated by knock-out strains engineered in the laboratory used to establish the functions of unknown genes. Inspired by this natural fine-scale microbial diversity, we show here that it can be used to develop hypotheses guiding biochemical experiments for establishing the role of these enzymes in nature. In this work, we investigated alginate degradation among closely related strains of the marine bacterium *Vibrio splendidus*. One strain, *V. splendidus* 13B01, exhibited high extracellular alginate lyase activity compared with other *V. splendidus* strains. To identify the enzymes responsible for this high extracellular activity, we compared *V. splendidus* 13B01 with the previously characterized *V. splendidus* 12B01, which has low extracellular activity and lacks two alginate lyase genes present in *V. splendidus* 13B01. Using a combination of genomics, proteomics, biochemical, and functional screening, we identified a polysaccharide lyase family 7 enzyme that is unique to *V. splendidus* 13B01, secreted, and responsible for the rapid digestion of extracellular alginate. These results demonstrate the value of querying the enzymatic repertoires of closely related microbes to rapidly pinpoint key proteins with beneficial functions.

Polysaccharide degradation by microbes represents one of the largest heterotrophic transformations of carbon-rich organic matter in the marine environment. Every year, marine algae transform ~45 gigatons of carbon dioxide from the atmosphere into biomass (1). Key constituents of algal biomass are glycans, which function as intracellular carbon/energy stores (2), cell wall building components (3), or secreted exudates (4). Glycans play a central role in the marine carbon cycle because they represent 30–80% of the total carbon content in algal matter, yet measurements of residual algal biomass in sinking particles obtained with sediment traps indicate that >99% of the autotrophic biomass that is produced at the surface, including the glycans, disappears throughout the water column (5–7). These results suggest that microbes, key decomposers of organic matter, have the capacity to efficiently deconstruct the wide variety of glycans produced by algae in the sea. However, most of the enzymes involved in the marine glycan cycle remain biochemically uncharacterized.

Microbes require multiple enzymes to deconstruct even the simplest glycan polysaccharides into simple sugars. These enzyme systems typically involve hydrolytic glycoside hydrolases or lytic polysaccharide lyases (PLs)[4] (www.cazy.org)[5] (8). Such enzyme systems have recently been described for a variety of algal polysaccharides (9–11). Alginate is a linear, carboxylated polysaccharide consisting of the mixed 1,4-linked epimers α-L-guluronate (G) and β-D-mannuronate (M), that is readily consumed by coastal microbial communities (12). It is one of the most abundant coastal polysaccharides and is found in the

This work was supported by Deutsche Forschungsgemeinschaft (DFG) Grant HE 7217/1-1 (to J.-H. H.) and United States Department of Energy, Office of Science, Office of Biological and Environmental Research, Award ER65474 (to M. F. P. and C. V. R.). The authors declare that they have no conflicts of interest with the contents of this article.

This article contains supplemental Tables S1–S3 and Figs. S1–S6.

[1] Both authors contributed equally to this work.

[2] To whom correspondence may be addressed: MARUM–Center for Marine Environmental Sciences, University of Bremen, Leobener Str. 8 D-28359 Bremen, Germany. Tel.: 49-421-218-65775; E-mail: jhhehemann@marum.de.

[3] To whom correspondence may be addressed: Dept. of Chemical and Biomolecular Engineering, University of Illinois at Urbana-Champaign, 600 S. Mathews Ave., Urbana, IL 61801. Tel.: 217-244-2247; Fax: 217-333-5052; E-mail: cvrao@illinois.edu.

[4] The abbreviations used are: PL, polysaccharide lyase; CBM32, family 32 carbohydrate-binding module; G, α-L-guluronate; M, β-D-mannuronate; qPCR, quantitative PCR; DP, degree of polymerization; TSB, tryptic soy broth; PDB, Protein Data Bank; TEAB, triethylammonium bicarbonate; NSAF, normalized spectral abundance factor; LCR, ligase cycling reaction; ESI, electrospray ionization.

[5] Please note that the JBC is not responsible for the long-term archiving and maintenance of this site or any other third party hosted site.

cell walls of brown seaweeds, such as kelp, that dominate primary production plant growth along the coasts of temperate marine provinces (13). Alginate has also been proposed as a renewable source for the production of biofuels (14, 15).

The enzymes involved in alginate degradation are known as alginate and oligoalginate lyases. They use β-elimination of the glycosidic bond to cleave alginate into smaller oligosaccharides or monomeric sugars (16, 17). They can be classified based on whether they preferentially degrade poly-M, poly-G, or poly-MG regions of alginate using either an endolytic or exolytic mechanism. In addition, the lyases can be secreted, membrane-bound, or intracellular. Many bacteria employ multiple alginate lyases to degrade alginate. A prime example is *Saccharophagus degradans* 2–40, which has 13 predicted alginate lyase genes (18), as well as other proteobacteria, including the Alteromonadales (19) and marine Flavobacteria, such as *Zobellia galactanivorans* (20).

A recent study investigated the ability of 55 closely related marine *Vibrionaceae* bacteria to degrade alginate (21). These bacteria were able to degrade extracellular alginate to varying degrees, with some growing best on short-chain (DP ~3–4) and others growing best on long-chain (DP >20) substrates. The behaviors were generally consistent among closely related strains except those within the *Vibrio splendidus* population, where significant diversity was observed. In particular, whereas all of the *V. splendidus* strains were able to grow well on short-chain substrates, only some grew well on long-chain substrates, and their growth rates and lag phases varied on these long-chain substrates. The ability to rapidly grow on long-chain substrates was attributed to enzyme secretion; strains that secrete alginate lyases grew much better than those that do not. Interestingly, the *V. splendidus* strains all exhibited similar levels of intracellular and membrane-bound alginate lyase activity, suggesting that some strains acquired additional lyases with high extracellular activity. These results are in line with a previous bioinformatics study revealing very high genotypic microdiversity of extracellular CAZymes, even among very closely related microbes (14).

In this work, we sought to identify the enzymes responsible for high secreted alginate lyase activity within the *V. splendidus* population. One strain, *V. splendidus* 13B01, was found to have significantly higher activity than the others, although they are indistinguishable by 16S RNA or other single-marker gene phylogenies. Using a combination of genomics, proteomics, biochemical, and functional screening, we identified a PL7 alginate lyase that is critical for rapid extracellular alginate breakdown. Our results demonstrate that differences in the enzyme repertoires between closely related strains can be used to rapidly pinpoint key proteins with beneficial functions.

Results

Activity screening reveals the diversity of alginate degradation within closely related V. splendidus strains

The alginate lyases have only been characterized in *V. splendidus* 12B01, which exhibits low extracellular lyase activity (15, 22). Therefore, we sought to identify the alginate lyases with high extracellular activity. As a first step, we screened the eight

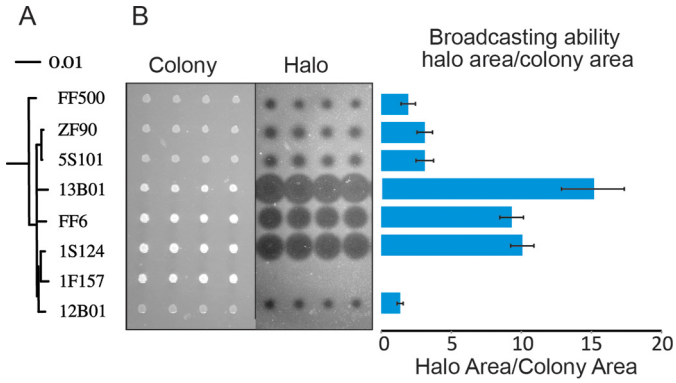

Figure 1. Comparison of secreted alginate lyase activity among closely related *V. splendidus* strains. *A*, phylogenetic comparison of closely related *V. splendidus* strains. The species tree was calculated as described previously with concatenated ribosomal proteins (21). *Scale bar*, substitutions per site. Notably, all of these strains can catabolize alginate (21). *B*, alginate lyase secretion assay on agar plates with marine broth medium supplemented with 0.25% alginate. The *Vibrio* strains were grown for 36 h, and the resulting colonies were imaged. Cetylpyridinium chloride revealed the dark halos indicative of alginate (*opaque background*) that was digested by secreted alginate lyase diffusing beyond the colony boundaries. The *bars* (*blue*; mean) and *error bars* (S.D.) were calculated from the four technical replicates shown in the *left panel*.

V. splendidus strains examined in a study by Hehemann *et al.* (21) for their ability to broadcast alginate lyase activity. Briefly, we grew the cells as individual colonies on agar plates supplemented with 0.25% alginate and then screened for secreted alginate lyase activity through the formation of dark halos.

Among the eight strains tested, *V. splendidus* 13B01 had the highest secreted activity, whereas the previously characterized *V. splendidus* 12B01 had the second lowest secreted activity (Fig. 1). Therefore, we focused on *V. splendidus* 13B01 due to its high extracellular alginate lyase activity. We next compared the growth of *V. splendidus* 12B01 and 13B01 on 1% alginate in liquid culture (supplemental Fig. S1). *V. splendidus* 13B01 grew 24% faster on alginate than *V. splendidus* 12B01 (0.51 h^{-1} *versus* 0.41 h^{-1}). These results confirm that *V. splendidus* 13B01 is better at catabolizing alginate than *V. splendidus* 12B01.

Comparative genomics reveals differences between alginate lyases in V. splendidus strains

Previous studies have suggested that rapid microbial adaptation to new environmental conditions or resources can result from gene transfer (21). Reconciliation of species and gene tree phylogenies revealed that *V. splendidus* 13B01 acquired an additional PL7 enzyme, which is lacking in 12B01 and which may account for the improved performance of 13B01 on long-chain alginate. To test this hypothesis, we compared the genomes of *V. splendidus* 12B01 and 13B01 to identify other genetic properties related to alginate metabolism that may account for the observed differences in alginate usage.

Both strains contain a homologous genetic island involved in alginate metabolism. *V. splendidus* 12B01 has four PL7 alginate lyases (PL7A, PL7B, PL7D, and PL7E) that are also present in *V. splendidus* 13B01. Phylogenetic analysis indicates that the four PL7 enzymes common to both *V. splendidus* 12B01 and *V. splendidus* 13B01 are closely related orthologs (sequence similarity >98%) (Fig. 2*A*). The PL7B, PL7D, and PL7E lyases contain one PL7 domain (Fig. 2*B*), whereas the PL7A lyase con-

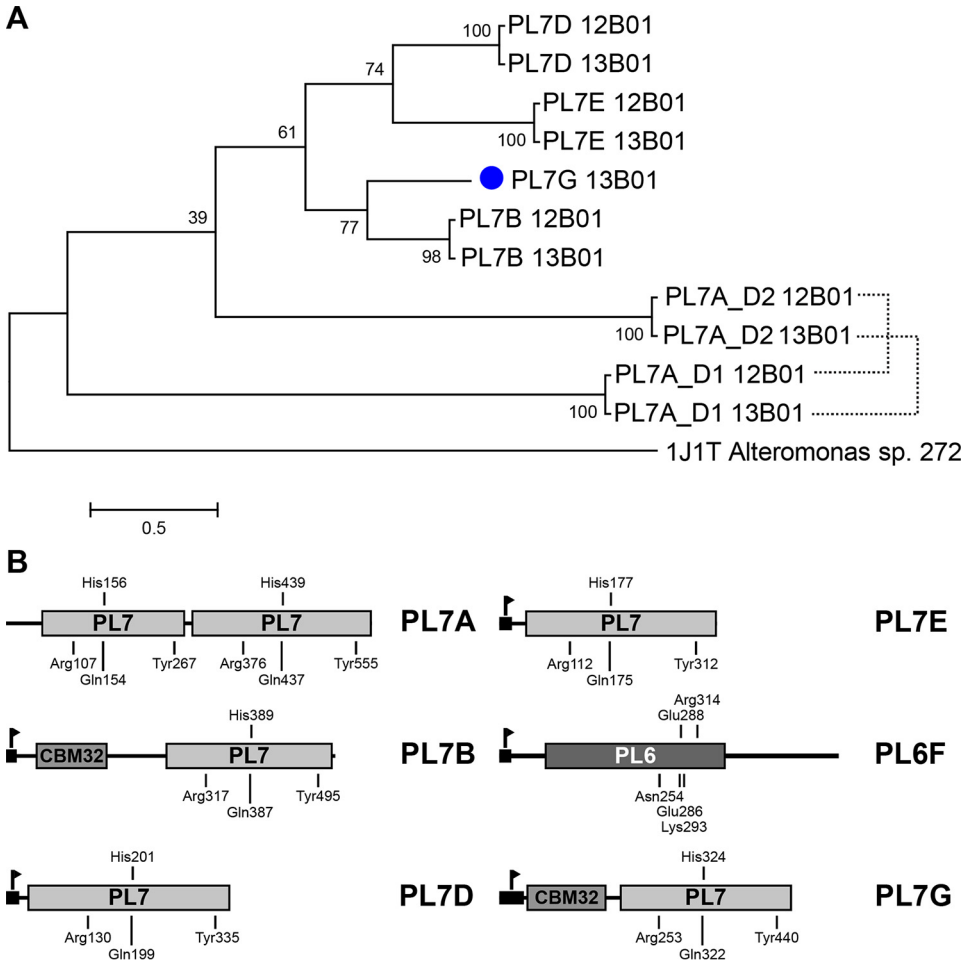

Figure 2. Alginate lyases in *V. splendidus* 12B01 and 13B01. *A*, rooted maximum likelihood tree of PL7 lyases in *V. splendidus* 12B01 and 13B01. The PL7 enzyme from *Alteromonas* sp. 272 was used as an outgroup. The *numbers* at nodes represent bootstrap values derived from 100 tree calculations. *B*, domain structure of alginate lyases in *V. splendidus* 13B01. The indicated amino acids are the hypothesized catalytic residues. CBM32 is the carbohydrate binding module family 32 domain. The *small flags* indicate signal peptides, where the *white* and *black boxes* are used specify whether these peptides are predicted to be cleaved by signal peptidase I or II, respectively. The signal peptides of secreted lyases are expected to be cleaved by signal peptidase I, and the signal peptides of membrane-associated lyases are expected to be cleaved by signal peptidase II (25, 49). The GenBank™ accession numbers are as follows: PL7A (OCH64533.1), PL7B (OCH64532.1), PL7D (OCH64519.1), PL7E (OCH62672.1), PL6F (OCH64519.1), and PL7G (OCH63958.1).

tains two PL7 domains, which are more distantly related to the other enzymes (16, 17).

V. splendidus 13B01, however, also has several unique features. First, it contains a PL7 alginate lyase, PL7G, not present in *V. splendidus* 12B01 and containing a single catalytic domain. This lyase is nested in a clade surrounded by the lyases PL7D, PL7B, and PL7E. Both PL7B and PL7G contain a family 32 carbohydrate-binding module (CBM32) in addition to their PL7 domain (23). Second, *V. splendidus* 13B01 also has a putative alginate lyase with a PL6 domain (16, 24). Both alginate lyases unique to *V. splendidus* 13B01, PL6F and PL7G, have the catalytic residues typical for PL6 and PL7 enzymes, suggesting that both are functional (24, 26, 27). These bioinformatics results suggest that PL6F, PL7G, or both may be responsible for the high extracellular lyase activity of *V. splendidus* 13B01.

Alginate-induced expression of PL7 and PL6 alginate lyase genes in 13B01

To ascertain the physiological response of the alginate lyase genes to alginate, we measured the expression of the alginate lyases in *V. splendidus* 13B01 using quantitative PCR (qPCR). Briefly, we grew cells in M9 minimal salt medium supplemented with 0.2% (w/v) glucose, 0.1% (w/v) alginate, or 1.0% (w/v) alginate and then harvested the mRNA during late exponential phase.

Growth on alginate induced expression of all alginate lyase genes relative to growth on glucose (Fig. 3). In particular, lyase gene expression at both alginate concentrations is induced >2-fold, with *pl7G* being induced >10-fold. Growth on 0.1 and 1.0% alginate yielded no discernable difference in gene expression for any of the six lyases. The lyases in *V. splendidus* 12B01 are also induced by alginate (22); however, they are expressed at a lower levels than their orthologues in *V. splendidus* 13B01. In addition, their expression is more tightly regulated because less expression occurs in the absence of alginate. Their expression also exhibits a more graded response to alginate, with less expression observed at lower alginate concentrations. Increased expression of the lyases at low alginate concentrations may explain why *V. splendidus* 13B01 grows better in liquid culture than *V. splendidus* 12B01.

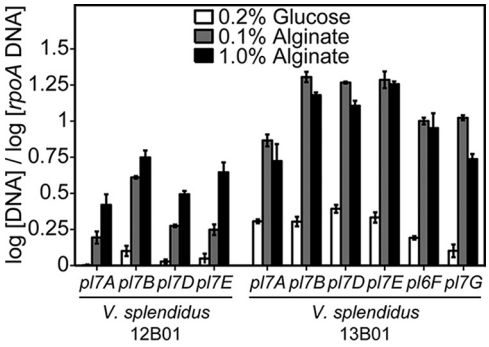

Figure 3. Expression of alginate lyases in *V. splendidus* 12B01 and 13B01 during growth on glucose and alginate as determined using quantitative PCR. The housekeeping gene *rpoA* was used as an internal control. The data for *V. splendidus* 12B01 were published previously (22) and are included for comparative purposes. *Bars*, mean of three technical replicates; *error bars*, S.D.

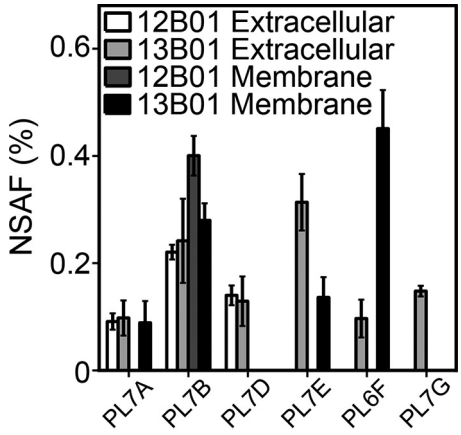

Figure 4. Comparison of alginate lyase expression and localization in *V. splendidus* 12B01 and 13B01 as determined by proteomics. *Bars*, mean of three technical replicates; *error bars*, S.D. The data are presented as NSAFs.

Protein localization and expression profiling using proteomics reveals that PL7G is the highly secreted alginate lyase

We next used proteomics to distinguish between the lyases enriched in the extracellular and membrane-bound fractions for *V. splendidus* 12B01 and 13B01. Liquid chromatography tandem mass spectrometry (LC-MS/MS) protein analysis revealed that the six alginate lyases in *V. splendidus* 13B01 were expressed during growth on alginate (Fig. 4) in agreement with the qPCR experiments (Fig. 3). Three (PL7A, PL7B, and PL7D) were detected in *V. splendidus* 12B01, but the fourth (PL7E) was below the detection limit. In general, we observed no significant differences in the distribution of the enzymes shared between *V. splendidus* 12B01 and 13B01. PL7A, PL7B, and PL7E were detected in both extracellular and membrane fractions. PL7D was only detected in the extracellular fraction. Among the enzymes unique to *V. splendidus* 13B01, PL6F was principally found in the membrane fraction, whereas PL7G was found solely in the extracellular fraction. These results are generally consistent with the predicted signal peptides for the *V. splendidus* 13B01 lyases (Fig. 2). The only discrepancy is with PL7E, which is predicted to be secreted but also found in the membrane fraction. Based on these results, we conclude that the high extracellular activity is most likely due to PL7G.

Recombinant production, purification, and characterization of V. splendidus 13B01 alginate lyases

We next tested the possibility that increased activity or altered specificity provides another source of physiological variation among the two *V. splendidus* strains. To examine the biochemical properties and substrate specificities of the alginate lyases, we produced the recombinant PL6 and PL7 enzymes from *V. splendidus* 13B01 in *E. coli* except PL7D, because it is identical to its previously characterized ortholog in *V. splendidus* 12B01 (22). Among the five enzymes, PL6F was the only soluble protein and could therefore be purified under native conditions, whereas the PL7 enzymes were found to be insoluble in inclusion bodies. To yield functional enzymes, we produced and purified the PL7 enzymes under denaturing conditions and then refolded them (supplemental Fig. S2). All of the lyases were stable and eluted as monomeric proteins in size exclusion chromatography (supplemental Fig. S3).

We first determined the optimal conditions for each lyase (supplemental Fig. S4). The lyases were found to have optimal activities over a range of pH values varying from 7.5 to 10. The optimal temperatures were between 20 and 25 °C, and the optimal NaCl concentrations were between 250 and 1000 mM. We also determined the enzymatic function of each of the two PL7A domains by producing each domain separately as a recombinant protein. We found that domain 2 of PL7A had 85% activity in comparison with the full PL7A enzyme, whereas domain 1 of PL7A had negligible enzymatic activity (supplemental Fig. S5), suggesting that it may have other functions, such as sugar binding. Similar results were reported for the two domains of PL7A from *V. splendidus* 12B01 (22).

We next determined the kinetic parameters for each lyase by measuring the activity at different alginate concentrations under optimal salt and pH conditions. All five alginate lyases exhibited Michaelis–Menten type kinetics (supplemental Fig. S6). The associated kinetic parameters are provided in Table 1. We observed some differences among the lyases common to *V. splendidus* 12B01 and 13B01. In general, the shared lyases are more active in *V. splendidus* 13B01, as determined by the enzymatic turnover number. However, these differences in the enzyme kinetics are not significant enough to explain the phenotypic differences (*e.g.* high secreted activity) between *V. splendidus* 12B01 and 13B01.

In the case of the alginate lyases unique to *V. splendidus* 13B01, we found that PL7G exhibits much stronger activity than PL6F. In fact, PL7G exhibits the highest turnover number among the six lyases. However, PL7G has a relatively low affinity for alginate, as indicated by its large K_m, suggesting that it is adapted to the high substrate concentrations present in marine alginate gels. Collectively, these results further suggest that the high extracellular activity of *V. splendidus* 13B01 is due to PL7G.

In addition to measuring the kinetic parameters, we also determined specificity of the lyases. Alginate is a polysaccharide consisting of the mixed 1,4-linked epimers, G and M. Different lyases can preferentially cleave the G–G, M–M, G–M, or M–G bonds in alginate. To determine the specificity of the *V. splendidus* 13B01 lyases, we measured the degradation products of

Table 1

Optimal environmental conditions and enzymatic kinetics of studied alginate lyases

The data and curve fits used to determine the *V. spendidus* 13B01 lyase kinetic parameters are found in supplemental Fig. S6. The *V. splendidus* 12B01 lyase parameters were previously determined (22). The kinetic parameters for PL7D in *V. splendidus* 13B01 were not determined because the enzyme is 100% identical to its homolog in *V. splendidus* 12B01.

		12B01	13B01
PL7A	pH	8.5	8.5
	Temperature (°C)	25	20
	NaCl (mM)	1000	750
	K_m (μM alginate)	36 ± 7	90 ± 30
	V_{max} (μM s^{-1})	0.13 ± 0.01	0.34 ± 0.02
	Turnover (s^{-1})	0.60 ± 0.02	1.9 ± 0.1
	Specificity	G-M	G-M
PL7B	pH	7.5	10.0
	Temperature (°C)	20-25	25
	NaCl (mM)	400	500
	K_m (μM alginate)	22 ± 5	150 ± 30
	V_{max} (μM s^{-1})	0.66 ± 0.06	0.76 ± 0.05
	Turnover (s^{-1})	3.7 ± 0.3	5.2 ± 0.3
	Specificity	G-M	G-M
PL7D	pH	8.0	Identical
	Temperature (°C)	20	
	NaCl (mM)	400	
	K_m (μM alginate)	60 ± 2	
	V_{max} (μM s^{-1})	0.52 ± 0.06	
	Turnover (s^{-1})	4.5 ± 0.5	
	Specificity	G-G	
PL7E	pH	7.5	10.0
	Temperature (°C)	25	20
	NaCl (mM)	400	1000
	K_m (μM alginate)	123 ± 6	170 ± 30
	V_{max} (μM s^{-1})	0.83 ± 0.02	1.50 ± 0.07
	Turnover (s^{-1})	7.1 ± 0.2	15.8 ± 0.7
	Specificity	G-G	G-G
PL6F	pH	No Homolog	8.5
	Temperature (°C)		20
	NaCl (mM)		250
	K_m (μM alginate)		40 ± 6
	V_{max} (μM s^{-1})		0.090 ± 0.002
	Turnover (s^{-1})		0.6 ± 0.1
	Specificity		G-M
PL7G	pH	No Homolog	7.5
	Temperature (°C)		25
	NaCl (mM)		500
	K_m (μM alginate)		300 ± 30
	V_{max} (μM s^{-1})		2.6 ± 0.1
	Turnover (s^{-1})		18.0 ± 0.7
	Specificity		M-G

alginate, mannuronate-enriched alginate, and guluronate-enriched alginate using ^{1}H NMR (Fig. 5). The results are summarized in Table 1. Among the shared lyases tested, no differences in specificity were detected. Among the unique lyases, PL6F exhibited G–M specificity, and PL7G exhibited M–G specificity. We also analyzed the degraded alginate products using ESI-MS and found that all lyases were endolytic (Fig. 6).

PL7G enables the high alginolytic performance of V. splendidus 13B01

Our data show that PL7G is the enzyme that probably differentiates *V. splendidus* 12B01 and 13B01 with regard to extracellular alginate degradation. In particular, it is unique to *V. splendidus* 13B01, has the highest activity, and is secreted. To further confirm this hypothesis, we deleted *pl7G* in *V. splendidus* 13B01. We then compared secreted alginate lyase activity in the wild type and the *pl7G* null mutant (Fig. 7). In support of our hypothesis, the *pl7G* mutant had significantly reduced (~8-fold) extracellular alginate lyase activity, similar to what is observed in *V. splendidus* 12B01. These results demonstrate that PL7G is principally responsible for the high extracellular alginate lyase activity of *V. splendidus* 13B01.

Discussion

Bacteria employ systems of complementary enzymes to degrade polymeric glycans into monosaccharides. Differences in the number of enzyme, due to loss, duplication, and transfer, in these glycan-degrading pathways have been documented even among closely related strains, suggesting that these changes reflect metabolic specialization. Indeed, a previous study was able to correlate the presence of different enzymes involved in alginate degradation in closely related coastal marine vibrios with their ability to grow on alginate substrates of varying chain length (21). Based on these results, the authors concluded that coastal vibrios have undergone an adaptive radiation that minimizes competition among closely related strains and creates an alginate degradation cascade involving three groups specialized for growth on substrates of different chain lengths and solubility (pioneers, harvesters, and scavengers).

In this work, we sought to identify the specific enzymes enabling this substrate specialization within the *V. splendidus* group. We focused specifically on the high extracellular lyase activity exhibited by some strains but not others. Those with high extracellular lyase activity are presumably specialized to grow on high–molecular weight substrates, such as alginate gels, whereas those with low extracellular activity are specialized for smaller–molecular weight substrates. As a first step, we compared the secreted lyase activity of eight related *V. splendidus* strains (Fig. 1). *V. splendidus* 13B01 exhibited the highest secreted lyase activity. Therefore, we sought to identify the specific lyases in *V. splendidus* 13B01 that enabled its high secreted lyase activity. This bacterium has six alginate lyases (Fig. 2). Four are shared with the previously characterized *V. splendidus* 12B01 (22), which exhibits low secreted lyase activity. Based on this difference, *V. splendidus* 12B01 was used as a reference point to develop hypotheses regarding the high secreted lyase activity of *V. splendidus* 13B01.

One question is whether the shared lyases are the same in these two strains. To address this question, we characterized the shared lyases. Whereas they exhibit higher activity in *V. splendidus* 13B01 than in *V. splendidus* 12B01 (Table 1), the increased activity was insufficient to explain differences in the ability to degrade extracellular alginate. We found instead, using a combination of genomic, proteomic, and biochemical approaches, that a single lyase, PL7G, present in *V. splendidus* 13B01 but not in *V. splendidus* 12B01, enables the high extracellular activity (Fig. 7). Removing PL7G from *V. splendidus* 13B01 by genetic manipulation created a knock-out strain that had the identical alginate lyase secretion phenotype as *V. splendidus* 12B01 when measured on our plate-based alginate lyase secretion assay. This result highlights the value of naturally occurring microdiversity to assign unknown functions to enzymes and/or other genes.

PL7G contains an N-terminal CBM32 domain (Fig. 2*B*). This domain is also present in PL7B. It is known to bind galactose, *N*-acetylglucosamine, lactose, and *N*-acetyl-D-lactosamine (28). Because it is present in some alginate lyases, it may also bind to alginate. Previous work demonstrated that removing a homolog of this domain from PL7B in *V. splendidus* 12B01

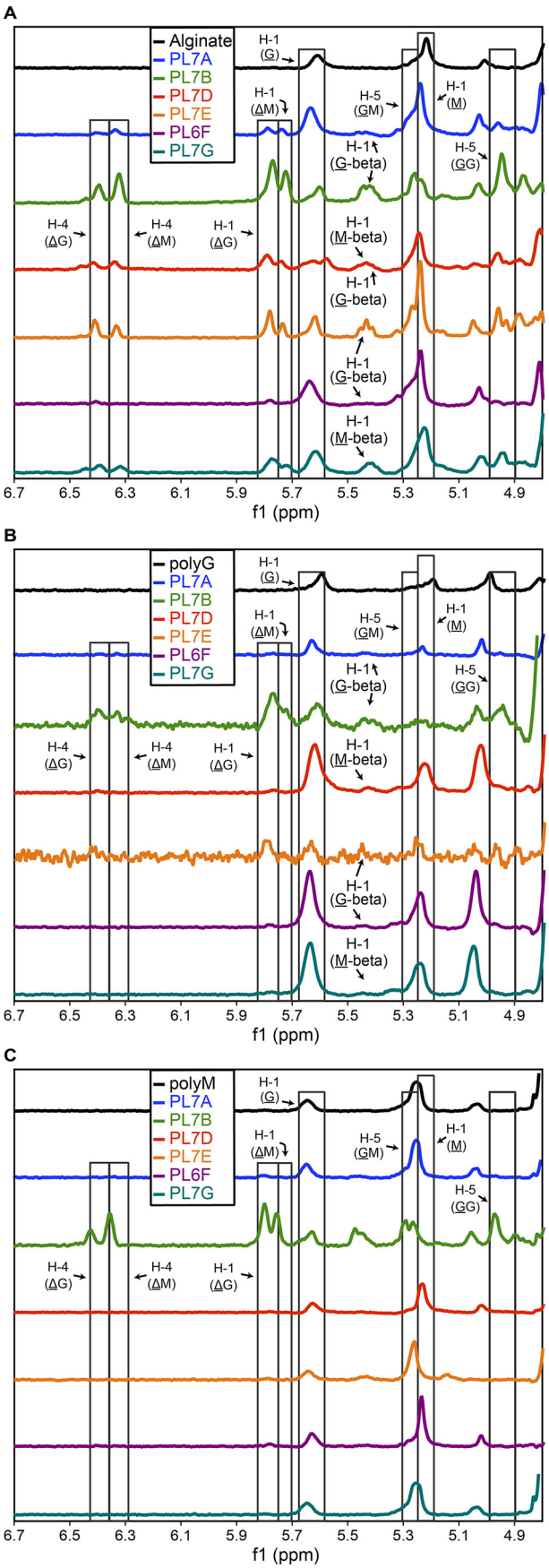

Figure 5. ^{1}H NMR (400-MHz) spectra of alginate and alginate-derived substrates following degradation with PL7A, PL7B, PL7D, PL7E, PL6F, and PL7G. *G* and *M*, signals from internal G and M residues, respectively; *G-beta* and *M-beta*, signals from reducing G and M residues, respectively; Δ, signal from 4-deoxy-L-erythro-hex-4-enepyranosyluronate non-reducing end residue. *Non-underlined residues* are the neighboring residues to those generating each signal. Protons (*H*) are *numbered* to indicate which particular proton causes the signal. *A*, alginate; *B*, poly-G–enriched alginate; *C*, poly-M–enriched alginate.

eliminated the activity (22), indicating that it is necessary for enzymatic function. However, others have found that removing this domain from an alginate lyase in *Vibrio algivorus* reduces but does not eliminate enzymatic activity (29). Although we did not explore the role of this domain in the present study, we suspect that it contributes to the ability of PL7G to degrade alginate gels. Indeed, carbohydrate-binding modules are known to enable enzymes to bind to insoluble glycans and modulate the specificity and activity of the cognate enzyme (30). Presumably, the CBM32 domain in PL7G serves a similar purpose by enabling the enzyme to attach to the alginate gels.

An additional question concerns the role of PL6F, the other lyase present in *V. splendidus* 13B01 but not in *V. splendidus* 12B01. This lyase exhibits relatively weak activity as compared with the other lyases. It is, however, expressed at a relative high level (Fig. 4), which could presumably compensate for its low activity. In addition, it appears to preferentially degrade large-molecular weight alginate, unlike the other lyases. In particular, the average degree of polymerization (DP) of its products, as determined by NMR, is 50 (supplemental Table S3). The other lyases yield products with significantly smaller DPs (all are <10 except PL7A, whose products have an average DP of 20). Because PL6F is preferentially localized to the membrane, this would suggest that it is used to degrade large alginate molecules, proximal to the cell, into smaller fragments accessible by the other membrane-localized enzymes, such as PL7B and PL7E. Assuming that this hypothesis is correct, then these results would suggest that the acquisition of PL6F further enables *V. splendidus* 13B01 to preferentially grow on high–molecular weight alginate substrates.

In addition to its high extracellular activity, *V. splendidus* 13B01 also exhibits a higher growth rate on alginate than *V. splendidus* 12B01. Whereas increased growth may be partially attributable to PL7G, we suspect that other factors are also involved. For one, *V. splendidus* 13B01 also exhibits a higher growth rate on glucose (supplemental Fig. S1), suggesting that its growth rate is intrinsically higher. However, the shared lyases also exhibit higher expression and activity, suggesting that this bacterium is better adapted to grow on alginate. Moreover, the additional lyases seem to be especially adapted to liquefy alginate gels because PL7G can rapidly penetrate into the gel medium during the alginate screening assay (Fig. 1). This may be attributable to its relatively high affinity constant, which indicates adaptation to the high substrate concentrations found in alginate gels (~1–2%, w/v). The use of such an enzyme supports the idea that *V. splendidus* 13B01 is a pioneer strain within the *Vibrio* group (21), enabling it to initiate the degradation of not yet colonized alginate-rich nutrient patches. Although such pioneers have an advantage on not yet colonized alginate gels, they may be outcompeted by strains like *V. splendidus* 12B01 when alginate particles become saturated with

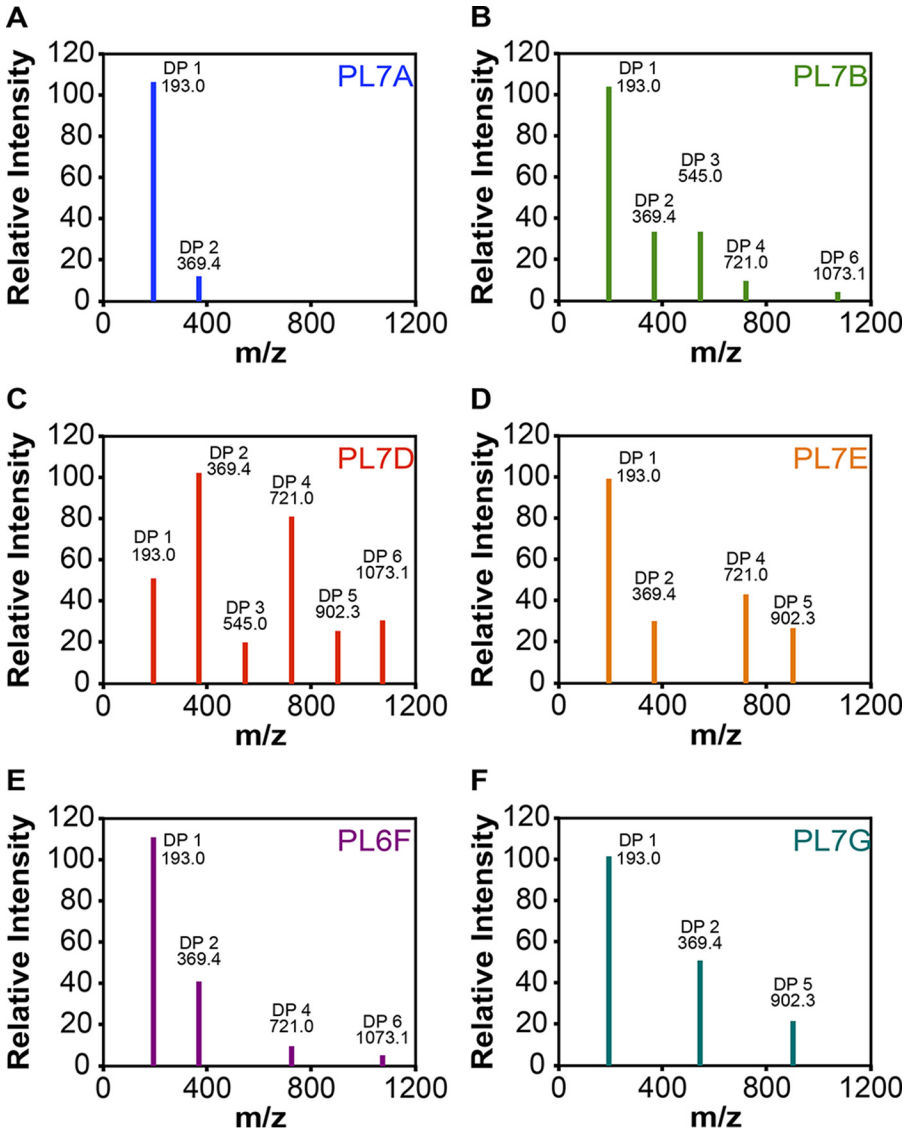

Figure 6. Negative-ion electrospray ionization mass spectra of alginate lyase-degraded alginate. DP and the respective integers (*1–6*) refer to the degree of polymerization. *m/z* values are listed *below* the DP values. Although the ESI-MS analysis of PL7A (*A*) only detected monomeric and dimeric degradation products, NMR shows that the actual product size has an average DP of 17 (data not shown). These longer-chain substrates are not detected by ESI-MS due to low signal intensity. The other lyases (*B–F*) are clearly endolytic, because ESI-MS analysis shows a ladder-type range of degradation products that is common for endo-acting enzymes degrading gel-forming, algal polysaccharides (9).

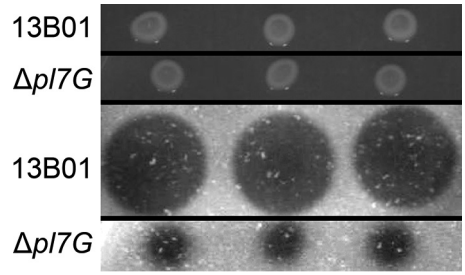

Figure 7. Comparison of secreted alginate lyase activities in wild-type *V. splendidus* 12B01 and 13B01 and a *V. splendidus* 13B01 Δ*pl7G* mutant. The *top three rows* show the colony images for the respective strains grown on a marine broth medium agar plate supplemented with 0.25% alginate. The *bottom three rows* show secreted alginate lyase activity of the same colonies, after they were manually removed, as determined by staining with cetylpyridinium chloride.

secreted lyases that solubilize the polymer. Under these conditions, the cost of secreting alginate lyases may decrease the fitness of strains like *V. splendidus* 13B01, suggesting niche differentiation according to the degradation state of alginate gels.

The results from the present study may have application in the productions of fuel and other chemical production using macroalgae. In particular, a recent study engineered *Escherichia coli* to produce ethanol from alginate using the alginate degradation pathway from *V. splendidus* 12B01 (15). To break down extracellular alginate into smaller oligomers capable of being taken up by the cell, the *E. coli* strain was also engineered to secrete a PL7 lyase from *Pseudoalteromonas* sp. SM0525. The native PL7 lyases from *V. splendidus* 12B01 were not considered. The results from the present study may aid in the design of bacteria capable of producing different fuels and chemicals from alginate by identifying the new lyases, PL6F and PL7G, that enable growth on high–molecular weight alginate substrates.

In conclusion, our results demonstrate the value of exploiting the evolutionary process for enzyme identification. In par-

ticular, evolution creates an array of closely related microbes, which behave like the mutants that one constructs in the laboratory when determining the function of unknown proteins. Our study shows that the analysis of closely related microbes in combination with suitable activity screens can reveal the function of unknown proteins, with the potential of leapfrogging the classical suite of molecular biology experiments.

Experimental procedures

Bacterial strains, media, and growth conditions

All cloning was performed in *E. coli* strain DH5α. Protein expression was performed in *E. coli* strain BL21(DE3). Conjugation was performed by mating with *E. coli* strain WM3064. *E. coli* was grown at 37 °C in Luria–Bertani (LB) medium (5 g/liter yeast extract, 10 g/liter tryptone, and 10 g/liter NaCl). Kanamycin was added at a concentration of 30 μg/ml. Diaminopimelate was supplemented at a concentration of 0.3 mM for experiments involving *E. coli* strain WM3064. *V. splendidus* 12B01 and 13B01 were isolated from particulate material obtained by filtering coastal waters (31). The strains were cultured in rich medium conditions on tryptic soy broth (TSB) (Difco) supplemented with 2% NaCl unless noted otherwise. Chloramphenicol was used at a concentration of 5 μg/ml. *V. splendidus* was grown at 20 °C in M9 minimal salt medium (32) (per liter of tap water: 11.28 g of M9 minimal salts (Sigma-Aldrich), 2 g of casamino acids, and 18 g of NaCl) unless noted otherwise. M9 minimal salt medium was then supplemented with 1 mM $MgSO_4$, 0.1 mM $CaCl_2$, and either 0.2% glucose, 0.1% alginate, or 1% alginate. Alginate was purchased from Sigma-Aldrich. Growth rates were determined by growing *V. splendidus* 12B01 and 13B01 overnight in M9 minimal salt medium and then subculturing to an A_{600} of 0.05 in fresh minimal medium. The increase in absorbance at 600 nm was then monitored.

Enzyme secretion

Cells, precultured for 24 h in 2216 marine medium (Difco), were plated in triplicate onto 2216 marine broth agar plates containing 0.25% (w/v) low-viscosity alginate (Sigma). The colonies were grown for 36 h at 20 °C and then imaged for colony size measurements. The colonies were removed by scraping the plate surface and washing with deionized water two times for 10 min. Lyase activity was determined by overlaying the agar plate with 10% (w/v) cetylpyridinium chloride (Sigma) in water for 20 min (33). The cetylpyridinium chloride solution was decanted, and the plate was washed twice with deionized water for a total of 20 min at 20 °C (34). The water was decanted, and lyase activity was revealed by the formation of cleared halos on an opaque background.

Phylogenetic analysis

An X-ray crystal structure-guided sequence alignment of the PL7 proteins was calculated with the previously published crystal structures of PL7 alginate lyases from *Sphingomonas* sp. A1 (PDB code 2CWS) (26) and *Alteromonas* sp. 272 (PDB code 1J1T) using ClustalW/T-coffee (35) as part of the Strap program (36). The alignment was calculated using default parameters. We included all protein sequences of *V. splendidus* 13B01 and 12B01 with PL7 domains. Because PL7A of *V. splendidus* 13B01 and 12B01 contained two PL7 domains, the domains were separated and treated as individual domains in the phylogenetic analysis. The structural alignment was plotted with Endscript to show the secondary structural elements of the associated PDB entries (37). Long inserts and N-terminal extensions, such as the CBM32 domains present in sequences of PL7B and PL7G, N-terminal signal peptides, and the C-terminal His tag of the sequence for 1J1T were manually removed from the alignment with Bioedit (38). This trimmed alignment, without the sequence 2CWS, was subsequently used to calculate the phylogenetic tree in Mega6 using the maximum likelihood method based on the JTT matrix-based model with default parameters and with 100 resamplings of the data set (39). The sequence of 1J1T, a PL7 alginate lyase from *Alteromonas* sp. 272, was used to root the tree.

Gene expression of alginate lyases

V. splendidus 13B01 was grown overnight in M9 minimal salt medium and then was subcultured 1:50 in fresh minimal medium. Samples were harvested at an A_{600} of 1.0. Total RNA was isolated using the RNeasy minikit (Qiagen). cDNA was then generated using the QuantiTect reverse transcription kit (Qiagen). The primers listed in supplemental Table S2 were then used to perform qPCR in triplicate. The primers were designed using Primer3Plus (www.bioinformatics.nl/primer3plus)[5] (40). qPCRs were performed using HotStart-IT SYBR Green qPCR Master Mix with UDG (Affymetrix) and a Bio-Rad MiniOpticon real-time PCR system (Bio-Rad). Serially diluted *V. splendidus* 13B01 genomic DNA was used to construct gene-dosing standards, and the 13B01 gene *rpoA* was used to control for differences in total mRNA (41).

Protein extraction for proteomic analysis

V. splendidus strains 12B01 and 13B01, respectively, were grown in triplicates in M9 minimal salt medium with 0.2% alginate as the carbon source (20 °C, 180 rpm). Bacterial cells were harvested at an A_{600} of 1.5 (after 7 h) at 9384 × *g* (4 °C, 15 min), washed twice in Tris-EDTA buffer (10 mM Tris-HCl, 10 mM EDTA), and stored at −80 °C until analysis. The supernatant, containing those *V. splendidus* proteins that were excreted into the extracellular medium (*i.e.* the extracellular protein fraction), was precipitated with 10% trichloroacetic acid (4 °C, overnight). Extracellular proteins were pelleted (9384 × *g*, 4 °C, 70 min), washed twice in 99% ethanol, and then resuspended in 50 mM triethylammonium bicarbonate (TEAB) buffer. *V. splendidus* cell pellets were resuspended in lysis buffer (50 mM Tris-HCl, Roche cOmplete protease inhibitor), and the cells were disrupted by sonication (Bandelin Sonopuls ultrasonic homogenizer, Berlin, Germany; 4 °C, 30% power, 0.5-s cycle, 3 × 30 s, 30-s pause). Crude cell debris was removed by centrifugation (8000 × *g*, 4 °C, 10 min), and the resulting raw protein extract was subjected to ultracentrifugation (100,000 × *g*, 4 °C, 70 min) to collect cellular membranes and associated proteins (*i.e.* the membrane fraction). Membrane proteins were extracted from the pellet by repeated solubilization and ultracentrifugation as described by Eymann *et al.* (42) and resuspended in 50 mM

TEAB buffer. Protein concentrations in the extracellular protein fraction and in the membrane fraction were determined according to Bradford (43) using the Nanoquant protein assay (Carl Roth, Karlsruhe, Germany).

LC-MS/MS analysis

Protein extracts (100 μg) were subjected to in-solution digestion, as described by Muntel *et al.* (44), at a final concentration of 1 μg/μl in 50 mM TEAB, 0.1% RapiGest (Waters, Milford, MA). After reduction (tris(2-carboxyethyl)phosphine, 5 mM final concentration) and alkylation (10 mM iodoacetamide), proteins were digested with trypsin (Promega, Madison, WI) for 6 h at 37 °C. RapiGest was removed by acidification and repeated centrifugation, and peptide mixtures were desalted using StageTips (Proxeon), according to the manufacturer's recommendations. Peptides were separated using reversed phase C18 column chromatography on a nanoACQUITY UPLC (Waters) before MS and MS/MS in an online-coupled LTQ-Orbitrap mass spectrometer (Thermo Fisher Scientific) (45). The SEQUEST® Sorcerer™ platform (Sage-N) was used for database searches of MS data against target-decoy protein sequence databases, containing the *V. splendidus* 12B01 and 13B01 sequences, respectively, and common laboratory contaminants. Peptide and protein identifications were validated in Scaffold version 4.2 (Proteome Software, Portland, OR) and filtered as described by Heinz *et al.* (46). Protein false discovery rates were 0.0% throughout all data sets. For label-free protein quantification, normalized spectral abundance factors (NSAFs) were calculated (47) from total spectrum counts as a measure of protein abundance. Only proteins that were identified in at least two of three replicates were included in the quantification. Relative protein abundance (*i.e.* a protein's proportion of all proteins in the same sample) was calculated as average NSAF% from the individual replicate NSAF% values ($n \geq 2$).

Plasmid construction

The alginate lyases from *V. splendidus* 13B01 were expressed from a T7 promoter using the overexpression plasmid pET-28(a). Each lyase was analyzed for the presence of a signal peptide using the SignalP version 4.1 server (http://www.cbs.dtu.dk/services/SignalP/)[5] (48) and the LipoP 1.0 server (http://www.cbs.dtu.dk/services/LipoP/)[5] (49). The signal peptides of PL7B, PL7E, PL6F, and PL7G were removed before cloning. The nucleotide sequence of each lyase can be found in supplemental Table S1. The overexpression vectors, pPL7A, pPL7B, and pPL7G, were constructed by amplifying the alginate lyase genes *pl7A*, *pl7B*, and *pl7G*, respectively, from *V. splendidus* 13B01 genomic DNA and then cloning these fragments into pET-28(a) using the restriction enzymes NcoI and XhoI. pPL6F was constructed by amplifying *pl6F* from *V. splendidus* 13B01 genomic DNA and cloning the fragment into pET-28(a) using the restriction enzymes NcoI and EagI. pPL7E was constructed in two steps. First, pET-28(a) was digested with restriction enzymes NcoI and EcoRI, the overhangs were filled in with Klenow fragment, and the blunt ends were ligated together to create a modified pET-28(a) lacking the N-terminal His tag, thrombin cleavage site, and T7 tag. *pl7E* was then amplified from *V. splendidus* 13B01 genomic DNA and cloned into the modified pET-28(a) using the restriction sites EcoRI and XhoI. Each of the overexpression vectors contains the alginate lyase gene with a C-terminal His_6 tag driven by an isopropyl β-D-1-thiogalactopyranoside-inducible T7 promoter. The alginate lyase domains of PL7A were independently amplified to include 5′-CTT TCC AGC-3′ upstream and 5′-TGT GGT CGT-3′ downstream of domain 1 and 5′-TCA AAC GAT-3′ upstream and 5′-GTT-3′ downstream of domain 2 and then cloned into pET-28(a) using the restriction enzymes NcoI and XhoI. When necessary, 5′-TT-3′ was included upstream of the cloned fragment to ensure that the fragment was in-frame with the C-terminal His_6 tag. Supplemental Table S2 contains the sequences for the oligonucleotides used in this work.

Protein purification and determination of molecular mass

Cells were grown overnight in LB medium and were supplemented with 1% glucose. Subcultures were then started in fresh medium and grown to an A_{600} of 0.5. Cells were cooled to 25 °C, and protein overexpression was then induced by adding isopropyl β-D-1-thiogalactopyranoside to a concentration of 1 mM. PL7E was grown for an additional 19 h at 25 °C. PL7A, PL7B, PL6F, and PL7G were grown for an additional 24 h at 16 °C. PL6F-expressing cells were lysed by suspending the cell pellet in native binding buffer (50 mM NaH_2PO_4, 300 mM NaCl, 10 mM imidazole, pH 8.0), and then lysozyme was added at 1 mg/ml and followed by incubation on ice for 30 min. The lysate was then sonicated six times for 10 s on ice. The PL6F lysate was clarified by centrifugation at 10,000 × *g* for 20 min and then passed through a 0.45-μm filter. PL6F was purified by loading the lysate onto two 5-ml HiTrap Chelating HP columns charged with 100 mM $NiSO_4$ and installed on an ÄKTA prime FPLC system (GE Healthcare). The columns were washed with 5 column volumes of wash buffer (50 mM NaH_2PO_4, 300 mM NaCl, 20 mM imidazole, pH 8.0), and then PL6F was eluted from the columns with 5 volumes of elution buffer (50 mM NaH_2PO_4, 300 mM NaCl, 250 mM imidazole, pH 8.0). PL7A-, PL7B-, PL7E-, and PL7G-containing cells were lysed by suspension in Buffer B (8 M urea, 100 mM NaH_2PO_4, 10 mM Tris-Cl, pH 8.0) and inverting the tubes at 25 °C for 1 h. The lysates were clarified by centrifugation at 9000 × *g* for 30 min and then passage through a 0.45-μm filter. The lyases were then loaded on two 5-ml HiTrap Chelating HP columns charged with 100 mM $NiSO_4$ installed on an ÄKTA prime FPLC system. The columns were then washed with 5 column volumes of Buffer C (8 M urea, 100 mM NaH_2PO_4, 10 mM Tris-Cl, pH 6.3). Each protein was then eluted with 5 volumes of Buffer D (8 M urea, 100 mM NaH_2PO_4, 10 mM Tris-Cl, pH 5.3). PL6F was dialyzed three times against TKMD-G (50) (50 mM Tris-Cl, pH 8.0, 5 mM MgCl, 50 mM KCl, 0.1 mM dithiothreitol, 10% glycerol, pH 8.0) at 4 °C for 2 h followed by an overnight charge at 4 °C. PL7A, PL7B, PL7D, PL7E, and PL7G were refolded via dialysis against TKMD-G three times at 4 °C for 2 h followed by an overnight charge at 4 °C.

Protein concentrations were determined using the Pierce BCA protein assay kit (Thermo Scientific) with albumin standards following the supplier's protocol. The native sizes of each protein were determined by size-exclusion high-performance liquid chromatography using a Shimadzu high-performance

liquid chromatography system that utilized an SPD-10A UV-visible detector set at 280 nm. A Bio-Sil SEC-250 column (300 × 7.8 mm) was then used to determine the native protein size using a mobile phase (50 mM Na_2HPO_4, 50 mM NaH_2PO4, and 150 mM NaCl, pH 6.8).

Alginate lyase activity assay

Alginate lyase reaction conditions were as follows. 0.25 μg of enzyme was added to 100 μl of APT buffer (20 mM sodium acetate, 20 mM monosodium phosphate, and 20 mM Tris base) containing 0.2% sodium alginate, unless noted otherwise. Each reaction was incubated for 20 min at the reported pH, temperature, and NaCl concentrations. The thiobarbituric assay was used to determine enzymatic activity (51, 52). 0.125 ml of 0.025 N H_2IO_6 in 0.125 N H_2SO_4 was added to each reaction mixture and then incubated for 20 min at 25 °C. Next, 0.25 ml of a 2% sodium arsenite in 0.5 N HCl solution was added and then incubated for 2 min. Finally, 1 ml of thiobarbituric acid (0.3%, pH 2) was added to the mixture and then heated at 100 °C for 10 min. The increase in absorbance at 548 nm was determined using a Shimadzu spectrophotometer. Activities were reported in 2-deoxy-D-glucose equivalent concentrations (53). The kinetic parameters were found by fitting the dose response activities to a Michaelis–Menten kinetic model. Enzyme calculations were based on the predicted mass of the enzymes. The predicted molecular masses of PL7A, PL7B, PL7D, PL7E, PL6F, and PL7G, were 65.1, 56.8, 38.2, 38.2, 59.2, and 50.8 kDa, respectively. The K_m toward alginate was determined assuming an alginate average chain length of 70.

Preparation of poly-G– and poly-M–enriched substrates

poly-G– and poly-M–enriched substrates were prepared as described previously (22) using the method of Chhatbar *et al.* (54). The M/G ratios, as determined by NMR, were 1.63 (alginate), 2.33 (poly-M), and 0.71 (poly-G).

^{1}H NMR analysis

Purified enzyme was mixed with 3 ml of 0.4% alginate solution in phosphate buffer (4.77 mM monosodium phosphate, 5.23 mM disodium phosphate, pH 7.6) and incubated at 25 °C for 3 h (55). The reaction mixture was dried using a refrigerated speed vacuum and then resuspended in 0.5 ml of deuterium oxide (D_2O). Samples were dried once more and then dissolved in 1 ml of D_2O. High-field ^{1}H NMR spectroscopy was accomplished using a Unity-Inova NMR 400-MHz system (Agilent, Santa Clara, CA), and data were collected at a temperature of 80 °C. Sample spinning, proton spectral width, number of scans, relaxation delay, proton pulse angle, and acquisition time were 20 Hz, −6 to 14 ppm, 256, 0 s, 40.99°, and 4.096 s, respectively. ^{1}H NMR results were analyzed using the method developed by Grasdalen (56) as described previously (22).

The average chain length of the alginate substrate, M/G ratio, and degree of polymerization of the lyase-degraded substrate were determined from ^{1}H NMR as discussed previously (57). Details are provided in supplemental Table S3.

Electrospray ionization mass spectroscopy

Electrospray ionization mass spectroscopy (Waters Quattro Ultima) was used to analyze the mass/charge ratios of the alginate lyase-degraded products. Positive- and negative-ionization modes were used. A solution containing 0.4% alginate in phosphate buffer, pH 7.6, was mixed with purified enzyme and incubated at 20 °C for 3 h. Samples were dried using a refrigerated speed vacuum, and 6 mg of the dried sample was dissolved in 1:1 MeOH-H_2O (10 pmol/ml) (58, 59) and injected into the electrospray. The mass range of the scans was from 100 to 1100 atomic mass units.

Gene knock-out

Knock-out of *pl7G* was conducted by use of a knock-out vector containing the region 1 kb upstream of *pl7G* fused to the region 1 kb downstream of *pl7G*. This vector was constructed in two steps. First, a ligase cycling reaction (LCR) (60) was used to fuse the two regions together in the vector pSW4426T (61) (a gift from Frédérique Le Roux). Linearized pSW4426T was generated with primers AB478F and AB478R by PCR. The upstream and downstream 1-kb regions of *pl7G* were amplified from the *V. splendidus* 13B01 genome with primers AB476F and AB476R and primers AB477F and AB477R, respectively. These three pieces were then phosphorylated with a T4 polynucleotide kinase reaction. The 55 ng/kb of each fragment was mixed with 5 μl of 20 mM ATP, 2 μl of 10× Ampligase buffer (Epicenter), 1 μl of T4 polynucleotide kinase (New England Biolabs), and H_2O to 20 μl. The mixture was then incubated for 1 h at 37 °C, followed by a deactivation for 20 min at 65 °C. The phosphorylated fragments were then ligated in an LCR. The 16.7 μl of the phosphorylated fragment mixture was mixed with 0.83 μl of 10× Ampligase buffer, 1 μl of Ampligase (Epicenter), 2 μl of 100% DMSO, 2.25 μl of betaine, 0.5 μl of 1.5 μM primers AB487F, AB490F, AB510F, and H_2O to 25 μl. The second step of the knock-out vector construction was subcloning the fused 1-kb upstream and downstream regions into the vector pJC4 (62). This was accomplished by amplifying the fused region from the LCR using primers AB513F and AB513R and subcloning this fragment into the vector pJC4 using the SpeI restriction site. The resulting vector, pPL7G-KO, contains the 1-kb *pl7G* upstream region fused to the 1-kb *pl7G* downstream region in the vector pJC4, which contains the $oriT_{RP4}$ transfer origin, the $oriR_{R6K\gamma}$ origin of replication, and the *sacB* gene for counterselection.

The knock-out vector pPL7G KO was conjugated from the *E. coli* strain WM3064 to *V. splendidus* 13B01 by the methods of Cordero *et al.* (62) with modification. Conjugation was performed by mixing 100 μl of each overnight-grown culture and washing once with TSB with 2% NaCl. The cells were then resuspended in 10 μl of TSB with 2% NaCl and spotted on TSB with 2% NaCl and 0.3 mM diaminopimelate solid medium. The plate was then incubated overnight at 30 °C. The cells were then removed and washed in TSB with 2% NaCl and plated on TSB with 2% NaCl and 5 μg/ml chloramphenicol. Colonies were then purified by streaking three times on TSB with 2% NaCl and chloramphenicol. The presence of the integrated vector was also verified. Integrants were then streaked once on TSB with 2% NaCl and then plated on fresh TSB with 1% NaCl and 5% sucrose to select for cells that have lost the integrated vector and *sacB* gene. The sucrose-resistant cells were then screened for loss of chloramphenicol resistance and loss of *pl7G*.

Author contributions—A. H. B., M. F. P., J.-H. H., and C. V. R. conceived and designed the study. A. H. B., M. J. P., and S. S. J. performed the cloning and expression, enzyme analysis, and gene expression experiments. A. H. B. and J.-H. H. performed the bioinformatics analysis. T. S., F. U., and S. M. performed the proteomics analysis. G. Y. performed the NMR and ESI-MS analysis. M. F. P. contributed the bacterial strains. A. H. B., S. S. J., J.-H. H., and C. V. R. wrote the paper. All authors approved the manuscript.

Acknowledgments—We thank Eric Alm for advice and suggestions. We also thank Kori Dunn for assistance with gel filtration. We thank Frédérique Le Roux, Santosh Koirala, Shuyan Zhang, and Charles Rutter for advice and suggestions regarding recombination protein production. We are indebted to Sebastian Grund and Dörte Becher for mass spectrometry measurements.

References

1. Falkowski, P. G., Barber, R. T., and Smetacek, V. V. (1998) Biogeochemical controls and feedbacks on ocean primary production. *Science* **281,** 200–207
2. Alderkamp, A. C., van Rijssel, M., and Bolhuis, H. (2007) Characterization of marine bacteria and the activity of their enzyme systems involved in degradation of the algal storage glucan laminarin. *FEMS Microbiol. Ecol.* **59,** 108–117
3. Torode, T. A., Marcus, S. E., Jam, M., Tonon, T., Blackburn, R. S., Hervé, C., and Knox, J. P. (2015) Monoclonal antibodies directed to fucoidan preparations from brown algae. *PLoS One* **10,** e0118366
4. Myklestad, S. M. (1995) Release of extracellylar products by phtyoplankton with special emphasis on polysaccharides. *Sci. Total Environ.* **165,** 155–164
5. Martin, J. H., Knauer, G. A., Karl, D. M., and Broenkow, W. W. (1987) VERTEX: carbon cycling in the northeast Pacific. *Deep Sea Res. A* **34,** 267–285
6. Iversen, M. H., Nowald, N., Ploug, H., Jackson, G. A., and Fischer, G. (2010) High resolution profiles of vertical particulate organic matter export off Cape Blanc, Mauritania: degradation processes and ballasting effects. *Deep Sea Res. I* **57,** 771–784
7. Hedges, J. I., Baldock, J. A., Gélinas, Y., Lee, C., Peterson, M., and Wakeham, S. G. (2001) Evidence for non-selective preservation of organic matter in sinking marine particles. *Nature* **409,** 801–804
8. Lombard, V., Golaconda Ramulu, H., Drula, E., Coutinho, P. M., and Henrissat, B. (2014) The carbohydrate-active enzymes database (CAZy) in 2013. *Nucleic Acids Res.* **42,** D490–D495
9. Hehemann, J. H., Correc, G., Thomas, F., Bernard, T., Barbeyron, T., Jam, M., Helbert, W., Michel, G., and Czjzek, M. (2012) Biochemical and structural characterization of the complex agarolytic enzyme system from the marine bacterium *Zobellia galactanivorans*. *J. Biol. Chem.* **287,** 30571–30584
10. Thomas, F., Barbeyron, T., Tonon, T., Génicot, S., Czjzek, M., and Michel, G. (2012) Characterization of the first alginolytic operons in a marine bacterium: from their emergence in marine Flavobacteriia to their independent transfers to marine Proteobacteria and human gut Bacteroides. *Environ. Microbiol.* **14,** 2379–2394
11. Hehemann, J. H., Kelly, A. G., Pudlo, N. A., Martens, E. C., and Boraston, A. B. (2012) Bacteria of the human gut microbiome catabolize red seaweed glycans with carbohydrate-active enzyme updates from extrinsic microbes. *Proc. Natl. Acad. Sci. U.S.A.* **109,** 19786–19791
12. Mitulla, M., Dinasquet, J., Guillemette, R., Simon, M., Azam, F., and Wietz, M. (2016) Response of bacterial communities from California coastal waters to alginate particles and an alginolytic *Alteromonas macleodii* strain. *Environ. Microbiol.* **18,** 4369–4377
13. Smith, S. V. (1981) Marine macrophytes as a global carbon sink. *Science* **211,** 838–840
14. Zimmerman, A. E., Martiny, A. C., and Allison, S. D. (2013) Microdiversity of extracellular enzyme genes among sequenced prokaryotic genomes. *ISME J.* **7,** 1187–1199
15. Wargacki, A. J., Leonard, E., Win, M. N., Regitsky, D. D., Santos, C. N., Kim, P. B., Cooper, S. R., Raisner, R. M., Herman, A., Sivitz, A. B., Lakshmanaswamy, A., Kashiyama, Y., Baker, D., and Yoshikuni, Y. (2012) An engineered microbial platform for direct biofuel production from brown macroalgae. *Science* **335,** 308–313
16. Garron, M. L., and Cygler, M. (2010) Structural and mechanistic classification of uronic acid-containing polysaccharide lyases. *Glycobiology* **20,** 1547–1573
17. Lombard, V., Bernard, T., Rancurel, C., Brumer, H., Coutinho, P. M., and Henrissat, B. (2010) A hierarchical classification of polysaccharide lyases for glycogenomics. *Biochem. J.* **432,** 437–444
18. Hutcheson, S. W., Zhang, H., and Suvorov, M. (2011) Carbohydrase systems of *Saccharophagus degradans* degrading marine complex polysaccharides. *Mar. Drugs* **9,** 645–665
19. Neumann, A. M., Balmonte, J. P., Berger, M., Giebel, H. A., Arnosti, C., Voget, S., Simon, M., Brinkhoff, T., and Wietz, M. (2015) Different utilization of alginate and other algal polysaccharides by marine *Alteromonas macleodii* ecotypes. *Environ. Microbiol.* **17,** 3857–3868
20. Zhu, Y., Thomas, F., Larocque, R., Li, N., Duffieux, D., Cladiere, L., Souchaud, F., Michel, G., and McBride, M. J. (2017) Genetic analyses unravel the crucial role of a horizontally acquired alginate lyase for brown algal biomass degradation by *Zobellia galactanivorans*. *Environ. Microbiol.* 10.1111/1462–2920.13699
21. Hehemann, J. H., Arevalo, P., Datta, M. S., Yu, X., Corzett, C. H., Henschel, A., Preheim, S. P., Timberlake, S., Alm, E. J., and Polz, M. F. (2016) Adaptive radiation by waves of gene transfer leads to fine-scale resource partitioning in marine microbes. *Nat. Commun.* **7,** 12860
22. Badur, A. H., Jagtap, S. S., Yalamanchili, G., Lee, J. K., Zhao, H., and Rao, C. V. (2015) Alginate lyases from alginate-degrading *Vibrio splendidus* 12B01 are endolytic. *Appl. Environ. Microbiol.* **81,** 1865–1873
23. Abbott, D. W., Eirín-López, J. M., and Boraston, A. B. (2008) Insight into ligand diversity and novel biological roles for family 32 carbohydrate-binding modules. *Mol. Biol. Evol.* **25,** 155–167
24. Michel, G., Pojasek, K., Li, Y., Sulea, T., Linhardt, R. J., Raman, R., Prabhakar, V., Sasisekharan, R., and Cygler, M. (2004) The structure of chondroitin B lyase complexed with glycosaminoglycan oligosaccharides unravels a calcium-dependent catalytic machinery. *J. Biol. Chem.* **279,** 32882–32896
25. Paetzel, M., Karla, A., Strynadka, N. C., and Dalbey, R. E. (2002) Signal peptidases. *Chem. Rev.* **102,** 4549–4580
26. Yamasaki, M., Ogura, K., Hashimoto, W., Mikami, B., and Murata, K. (2005) A structural basis for depolymerization of alginate by polysaccharide lyase family-7. *J. Mol. Biol.* **352,** 11–21
27. Han, Y. H., Garron, M. L., Kim, H. Y., Kim, W. S., Zhang, Z., Ryu, K. S., Shaya, D., Xiao, Z., Cheong, C., Kim, Y. S., Linhardt, R. J., Jeon, Y. H., and Cygler, M. (2009) Structural snapshots of heparin depolymerization by heparin lyase I. *J. Biol. Chem.* **284,** 34019–34027
28. Ficko-Blean, E., and Boraston, A. B. (2006) The interaction of a carbohydrate-binding module from a *Clostridium perfringens N*-acetyl-β-hexosaminidase with its carbohydrate receptor. *J. Biol. Chem.* **281,** 37748–37757
29. Doi, H., Tokura, Y., Mori, Y., Mori, K., Asakura, Y., Usuda, Y., Fukuda, H., and Chinen, A. (2017) Identification of enzymes responsible for extracellular alginate depolymerization and alginate metabolism in *Vibrio algivorus*. *Appl. Microbiol. Biotechnol.* **101,** 1581–1592
30. Boraston, A. B., Bolam, D. N., Gilbert, H. J., and Davies, G. J. (2004) Carbohydrate-binding modules: fine-tuning polysaccharide recognition. *Biochem. J.* **382,** 769–781
31. Hunt, D. E., David, L. A., Gevers, D., Preheim, S. P., Alm, E. J., and Polz, M. F. (2008) Resource partitioning and sympatric differentiation among closely related bacterioplankton. *Science* **320,** 1081–1085
32. Gómez-León, J., Villamil, L., Lemos, M. L., Novoa, B., and Figueras, A. (2005) Isolation of *Vibrio alginolyticus* and *Vibrio splendidus* from aquacultured carpet shell clam (*Ruditapes decussatus*) larvae associated with mass mortalities. *Appl. Environ. Microbiol.* **71,** 98–104

33. Gacesa, P., and Wusteman, F. S. (1990) Plate assay for simultaneous detection of alginate lyases and determination of substrate specificity. *Appl. Environ. Microbiol.* **56,** 2265–2267
34. MacDonald, L. C., and Berger, B. W. (2014) A polysaccharide lyase from *Stenotrophomonas maltophilia* with a unique, pH-regulated substrate specificity. *J. Biol. Chem.* **289,** 312–325
35. Armougom, F., Moretti, S., Poirot, O., Audic, S., Dumas, P., Schaeli, B., Keduas, V., and Notredame, C. (2006) Expresso: automatic incorporation of structural information in multiple sequence alignments using 3D-Coffee. *Nucleic Acids Res.* **34,** W604–W608
36. Gille, C., and Frommel, C. (2001) STRAP: editor for STRuctural Alignments of Proteins. *Bioinformatics* **17,** 377–378
37. Robert, X., and Gouet, P. (2014) Deciphering key features in protein structures with the new ENDscript server. *Nucleic Acids Res.* **42,** W320–W324
38. Hall, T. A. (1999) BioEdit: a user-friendly biological sequence alignment editor and analysis program for Windows 95/98/NT. *Nucleic Acids Symp. Ser.* **41,** 95–98
39. Tamura, K., Stecher, G., Peterson, D., Filipski, A., and Kumar, S. (2013) MEGA6: Molecular Evolutionary Genetics Analysis version 6.0. *Mol. Biol. Evol.* **30,** 2725–2729
40. Rozen, S., and Skaletsky, H. (2000) Primer3 on the WWW for general users and for biologist programmers. *Methods Mol. Biol.* **132,** 365–386
41. Jagtap, S. S., Hehemann, J. H., Polz, M. F., Lee, J. K., and Zhao, H. (2014) Comparative biochemical characterization of three exolytic oligoalginate lyases from *Vibrio splendidus* reveals complementary substrate scope, temperature, and pH adaptations. *Appl. Environ. Microbiol.* **80,** 4207–4214
42. Eymann, C., Dreisbach, A., Albrecht, D., Bernhardt, J., Becher, D., Gentner, S., Tam le, T., Büttner, K., Buurman, G., Scharf, C., Venz, S., Völker, U., and Hecker, M. (2004) A comprehensive proteome map of growing *Bacillus subtilis* cells. *Proteomics* **4,** 2849–2876
43. Bradford, M. M. (1976) A rapid and sensitive method for the quantitation of microgram quantities of protein utilizing the principle of protein-dye binding. *Anal. Biochem.* **72,** 248–254
44. Muntel, J., Hecker, M., and Becher, D. (2012) An exclusion list based label-free proteome quantification approach using an LTQ Orbitrap. *Rapid Commun. Mass Spectrom.* **26,** 701–709
45. Xing, P., Hahnke, R. L., Unfried, F., Markert, S., Huang, S., Barbeyron, T., Harder, J., Becher, D., Schweder, T., Glöckner, F. O., Amann, R. I., and Teeling, H. (2015) Niches of two polysaccharide-degrading *Polaribacter* isolates from the North Sea during a spring diatom bloom. *ISME J.* **9,** 1410–1422
46. Heinz, E., Williams, T. A., Nakjang, S., Noël, C. J., Swan, D. C., Goldberg, A. V., Harris, S. R., Weinmaier, T., Markert, S., Becher, D., Bernhardt, J., Dagan, T., Hacker, C., Lucocq, J. M., Schweder, T., *et al.* (2012) The genome of the obligate intracellular parasite *Trachipleistophora hominis*: new insights into microsporidian genome dynamics and reductive evolution. *PLoS Pathog.* **8,** e1002979
47. Zybailov, B., Mosley, A. L., Sardiu, M. E., Coleman, M. K., Florens, L., and Washburn, M. P. (2006) Statistical analysis of membrane proteome expression changes in *Saccharomyces cerevisiae*. *J. Proteome Res.* **5,** 2339–2347
48. Petersen, T. N., Brunak, S., von Heijne, G., and Nielsen, H. (2011) SignalP 4.0: discriminating signal peptides from transmembrane regions. *Nat. Methods* **8,** 785–786
49. Juncker, A. S., Willenbrock, H., Von Heijne, G., Brunak, S., Nielsen, H., and Krogh, A. (2003) Prediction of lipoprotein signal peptides in Gram-negative bacteria. *Protein Sci.* **12,** 1652–1662
50. Yuan, W., Glekas, G. D., Allen, G. M., Walukiewicz, H. E., Rao, C. V., and Ordal, G. W. (2012) The importance of the interaction of CheD with CheC and the chemoreceptors compared to its enzymatic activity during chemotaxis in *Bacillus subtilis*. *PLoS One* **7,** e50689
51. Preiss, J., and Ashwell, G. (1962) Alginic acid metabolism in bacteria. I. Enzymatic formation of unsaturated oligosaccharides and 4-deoxy-L-erythro-5-hexoseulose uronic acid. *J. Biol. Chem.* **237,** 309–316
52. Weissbach, A., and Hurwitz, J. (1959) The formation of 2-keto-3-deoxyheptonic acid in extracts of *Escherichia coli* B. I. Identification. *J. Biol. Chem.* **234,** 705–709
53. Ryu, M., and Lee, E. Y. (2011) Saccharification of alginate by using exolytic oligoalginate lyase from marine bacterium *Sphingomonas* sp. MJ-3. *J. Ind. Eng. Chem.* **17,** 853–858
54. Chhatbar, M., Meena, R., Prasad, K., and Siddhanta, A. K. (2009) Microwave assisted rapid method for hydrolysis of sodium alginate for M/G ratio determination. *Carbohydr. Polymers* **76,** 650–656
55. Kam, N., Park, Y. J., Lee, E. Y., and Kim, H. S. (2011) Molecular identification of a polyM-specific alginate lyase from *Pseudomonas* sp. strain KS-408 for degradation of glycosidic linkages between two mannuronates or mannuronate and guluronate in alginate. *Can. J. Microbiol.* **57,** 1032–1041
56. Grasdalen, H. (1983) High-field, 1H-n.m.r. spectroscopy of alginate: sequential structure and linkage conformations. *Carbohydr. Res.* **118,** 255–260
57. Ertesvåg, H., Erlien, F., Skjåk-Braek, G., Rehm, B. H., and Valla, S. (1998) Biochemical properties and substrate specificities of a recombinantly produced *Azotobacter vinelandii* alginate lyase. *J. Bacteriol.* **180,** 3779–3784
58. Lundqvist, L. C., Jam, M., Barbeyron, T., Czjzek, M., and Sandström, C. (2012) Substrate specificity of the recombinant alginate lyase from the marine bacteria *Pseudomonas alginovora*. *Carbohydr. Res.* **352,** 44–50
59. Zhang, Z., Yu, G., Guan, H., Zhao, X., Du, Y., and Jiang, X. (2004) Preparation and structure elucidation of alginate oligosaccharides degraded by alginate lyase from *Vibro* sp. 510. *Carbohydr. Res.* **339,** 1475–1481
60. Yu, N. Y., Wagner, J. R., Laird, M. R., Melli, G., Rey, S., Lo, R., Dao, P., Sahinalp, S. C., Ester, M., Foster, L. J., and Brinkman, F. S. L. (2010) PSORTb 3.0: improved protein subcellular localization prediction with refined localization subcategories and predictive capabilities for all prokaryotes. *Bioinformatics* **26,** 1608–1615
61. Le Roux, F., Binesse, J., Saulnier, D., and Mazel, D. (2007) Construction of a *Vibrio splendidus* mutant lacking the metalloprotease gene *vsm* by use of a novel counterselectable suicide vector. *Appl. Environ. Microbiol.* **73,** 777–784
62. Cordero, O. X., Wildschutte, H., Kirkup, B., Proehl, S., Ngo, L., Hussain, F., Le Roux, F., Mincer, T., and Polz, M. F. (2012) Ecological populations of bacteria act as socially cohesive units of antibiotic production and resistance. *Science* **337,** 1228–1231

Exploiting fine-scale genetic and physiological variation of closely related microbes to reveal unknown enzyme functions

Ahmet H. Badur, Matthew J. Plutz, Geethika Yalamanchili, Sujit Sadashiv Jagtap, Thomas Schweder, Frank Unfried, Stephanie Markert, Martin F. Polz, Jan-Hendrik Hehemann and Christopher V. Rao

J. Biol. Chem. 2017, 292:13056-13067.
doi: 10.1074/jbc.M117.787192 originally published online June 7, 2017